Braz J Phys (2014) 44:658–664
DOI 10.1007/s13538-014-0250-6

SOCIEDADE BRASILEIRA DE FÍSICA

CONDENSED MATTER

Using Polarization to Control the Phase of Spatial Modes for Application in Quantum Information

W. F. Balthazar · D. P. Caetano · C. E. R. Souza · J. A. O. Huguenin

Received: 15 April 2014 / Published online: 19 August 2014

Abstract Exploiting spatial modes and polarization, we experimentally demonstrate the realization of a conditional π-phase shift. Our approach is based on an optical circuit where the polarization and transverse degrees of freedom control the Gouy phase which is applied on Hermite-Gaussian beams. Our results show good agreement with the simulation of the optical circuit. As an application, we propose the implementation of a two-qubit quantum phase gate, where the qubits are encoded on the Hermite-Gaussian modes and linear polarization states.

Keywords Conditional phase shift · Two-qubit phase gate · Quantum information

W. F. Balthazar
Programa de Pós-Graduação em Física and Instituto de Ciências Exatas, Universidade Federal Fluminense, Volta Redonda, Rio de Janeiro, Brazil
e-mail: wagnerbalthazar@if.uff.br

D. P. Caetano
Escola de Engenharia Industrial Metalúrgica de Volta Redonda, Universidade Federal Fluminense, Volta Redonda, Rio de Janeiro, Brazil
e-mail: dpcaetano@id.uff.br

C. E. R. Souza · J. A. O. Huguenin (✉)
Instituto de Ciências Exatas and Programa de Pós-Graduação em Física, Universidade Federal Fluminense, Niterói, Rio de Janeiro, Brazil
e-mail: jose_huguenin@id.uff.br

C. E. R. Souza
e-mail: carloseduardosouza@id.uff.br

1 Introduction

Spatial modes of the electromagnetic field have been exploited as an interesting degree of freedom for fundamental works on nonlinear optics [1, 2] and quantum optics [3, 4]. In the quantum information scenario, the preparation of two-qubit states has been the subject of investigation, in particular, due to its importance for implementing quantum gates. For a single-photon field, two qubits have been encoded using two distinct degrees of freedom, namely spatial modes and polarization. Using the longitudinal spatial modes and polarization, it has been demonstrated the generation and characterization of single-photon two-qubit entangled states [5] as well as the implementation of a deterministic controlled-NOT gate [6]. By using transverse spatial modes and polarization, new approaches for implementing controlled-NOT gates [7–9], experimental realization of the Deutsch algorithm [10], and implementation of quantum key distribution systems [11] have been reported. The transference of quantum information between polarization and transverse mode degrees of freedom was proposed and experimentally demonstrated [12]. Recently, two-qubit states encoded in transverse modes and polarization have been applied for experimental realization of a quantum game, namely the quantum prisoners dilemma [13].

Hermite–Gauss (HG) and Laguerre–Gauss (LG) are important examples of transverse spatial modes used to describe light beams. An interesting property of the first-order HG and LG modes is the fact that they have a geometrical representation similar to Poincaré sphere used to describe polarization states [14]. For Hermite–Gaussian

beams propagating along z-direction, the field distribution is given by

$$HG_{1,0}(x,y,z) = \sqrt{\frac{2}{\pi}}\frac{2x}{w^2(z)}\exp\left(-\frac{x^2+y^2}{w^2(z)}\right) \times \exp\left\{i\left[\frac{k\,(x^2+y^2)}{2R(z)} + \arctan\left(\frac{z}{z_R}\right)\right]\right\}, \quad (1)$$

$$HG_{0,1}(x,y,z) = \sqrt{\frac{2}{\pi}}\frac{2y}{w^2(z)}\exp\left(-\frac{x^2+y^2}{w^2(z)}\right) \times \exp\left\{i\left[\frac{k\,(x^2+y^2)}{2R(z)} + \arctan\left(\frac{z}{z_R}\right)\right]\right\}, \quad (2)$$

where $w(z) = \sqrt{w_0^2(1+z/z_R)}$ is the width of the beam, with w_0 being its waist, z_R is the Rayleigh length, $R(z)$ is the wave front radius, and the phase factor $\exp(i \arctan z/z_R)$ is a longitudinal phase, so-called Gouy phase [15, 16]. For a Gaussian beam passing through a lens, the Gouy phase can be observed along the propagation around the focal plane of the lens. The Gouy phase has important applications and its physical origins is discussed in Ref. [17].

In this work, we exploit the Gouy phase acquired by Hermite–Gaussian beams to propose and experimentally demonstrate an optical circuit to control the phase of transverse spatial modes using polarization. Here, the polarization and spatial modes degrees of freedom determine the optical state that will acquire the Gouy phase. In Section 2, we introduce the optical circuit in detail. Section 3 presents the experimental results and the corresponding discussions. In Section 4, we show how our scheme can be applied for implementing a two-qubit quantum phase gate. Finally, in Section 5, we present our conclusions.

2 Conditional Phase Control

The core of our proposal is the Gouy phase acquired by Hermite–Gaussian modes passing into an astigmatic mode converter depending on the polarization state. The well-known Gouy phase [15] can be observed when a laser beam is focused. An isotropically focused Hermite-Gaussian mode $HG_{m,n}(x,y,z)$ propagating along the $z-$direction has the Gouy phase given by

$$\Phi_{m,n} = (m+n+1)arctan(\frac{z}{z_R}). \quad (3)$$

The Rayleigh length z_R is equal for the transverse direction in the isotropic case. For an astigmatic beam, the Rayleigh length is different for transverse orthogonal directions ($z_{Rx} \neq z_{Ry}$) which lead us to the following Gouy phase

$$\Phi_{m,n} = (m+\frac{1}{2})\phi_x + (n+\frac{1}{2})\phi_y, \quad (4)$$

with $\phi_\alpha = arctan(z/z_\alpha)$, $\alpha = x, y$. Cylindrical lens naturally produces this kind of astigmatism and it is exploited to construct the astigmatic mode converter, largely used to convert first-order Hermitian-Gaussian into Laguerre-Gaussian beams and vice versa [18].

Figure 1 shows the basic scheme of the mode converter. Two identical cylindrical lenses with focal length f are positioned at a distance d from each other. The direction along the longer part of the cylindrical lens defines the orientation of the converter. This direction can be rotated by an angle θ with respect to the horizontal (x-direction). Note that the beam is astigmatic only in the region between the lenses.

From (4), we can easily understand the different Gouy phases acquired by different orders of Hermitian-Gaussian beams in an astigmatic mode converter due to the difference between ϕ_x and ϕ_y. In addition, the amount of acquired phase Φ depends on the distance between the lens and it can vary continuously with respect to this parameter.

The matrix formalism is very useful to describe the action of the astigmatic converter on the HG modes. The matrix for the converter ϕ oriented at $\theta = 0$ with respect to the horizontal $C(0,\phi)$ presented in Ref. [19] can be generalized by using the rotation matrix $R(\theta)$ as

$$C(\theta,\phi) = R(\theta)C(0,\phi)R(-\theta), \quad (5)$$

leading us to

$$C(\theta,\phi) = \begin{bmatrix} \cos^2(\theta) + e^{i\phi}\sin^2(\theta) & (e^{i\phi}-1)\sin(\theta)\cos(\theta) \\ (e^{i\phi}-1)\sin(\theta)\cos(\theta) & \sin^2(\theta) + e^{i\phi}\cos^2(\theta) \end{bmatrix} \quad (6)$$

where θ is the converter orientation and ϕ is the Gouy phase imprinted by the mode converter. The most common mode converters are the $\pi/2$ and the π type [18]. The $\pi/2$ type is obtained positioning the lens at distance $d = \sqrt{2}f$. This converter introduces a phase difference of $\pi/2$ between the $HG_{0,1}$ and $HG_{1,0}$. It is used to convert HG mode into LG mode. The π type converter introduces a phase difference of π between $HG_{0,1}$ and $HG_{1,0}$. This converter is obtained by setting $d = 2f$ and it can be used to convert Laguerre-Gaussian beam LG_0^{+1} into LG_0^{-1}.

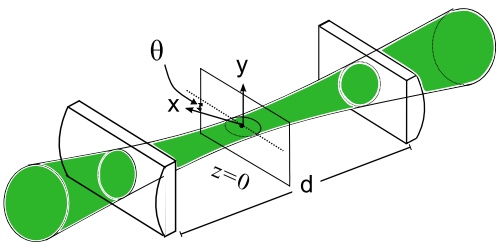

Fig. 1 Configuration of the astigmatic mode converter

For the case in which $HG_{0,1}$ and $HG_{1,0}$ are passing through $C(0,\pi)$, we can write

$$C(0,\pi)HG_{1,0} = HG_{0,1},$$
$$C(0,\pi)HG_{0,1} = e^{i\pi}HG_{0,1}. \quad (7)$$

By adding a polarization degree of freedom in the base $\{H, V\}$ to (7), we can perform a conditional phase shifting in the first-order Hermite-Gaussian beam.

Next, let us describe how the conditional phase shift can be experimentally performed. The experimental setup is presented in Fig. 2. A horizontally polarized laser beam with wavelength of 532 nm, 10 mW power, pass into a polarized beam splitter ($PBS-1$) in order to reject spurious vertical polarization components and to prepare the beam possessing horizontal polarization (H). The beam pass into a holographic mask in order to produce the transverse mode $HG_{1,0}$ referred as h-mode. This mode is filtered in a spatial filter producing a HG-mode with diameter around 2.0 mm. A half-wave Plate (HWP) is used to set the beam polarization. Setting the fast axes of the HWP at 0° with respect to the horizontal, the laser beam has H-polarization and h-mode, referred as Hh mode. Rotating the HWP by 45°, we convert the H into V polarization, producing the Vh mode. In order to obtain the states associated with the HG_{01} called spatial mode v, we can rotate the mask by an angle of 90°. Setting the HWP at 0° and 45°, we produce the modes Hv and Vv.

The conditional phase control of the spatial modes is performed by the optical circuit G. The mode Hh and Hv are transmitted by the $PBS-2$, and they do not pass trough the $\pi-$mode converter. The modes Vh and Vv are reflected by the $PBS-2$ and pass trough the $\pi-$mode converter composed of two cylindrical lens with dimensions of $12.7 \times 25.4\ mm$ possesing a focal lengh $f = 12.5\ mm$. By (7) only the mode Vv acquires the π-phase. The $PBS-3$ recombines the two arms.

In order to compare the phase difference between the beam passing trough the $\pi-$mode converter and the free propagating beam, a reference beam is needed. A balanced beam splitter ($BS-1$), placed immediately after the mode preparation, separates the reference and the mode sent into the optical circuit.

The output of the circuit G will interfere with the reference beam in a second balanced beam splitter ($BS-2$), the interference patterns are projected in a plane, and the image of the interference fringes is recorded by the CCD camera.

3 Experimental Results and Discussion

The experiment was performed using the experimental setup showed in Fig. 2. Initially, we verify the conditional phase shift for the modes Hh and Hv, corresponding to a first data set. The results are shown in Fig. 3. The intensity profiles are shown in Fig. 3a and b, corresponding to the modes Hh and Vh, respectively. The interference patterns are shown in Fig. 3c and d, where the dashed line is a guide to the eyes. It can be seen that the center of both interference patterns present bright fringes. This result indicates that no relative Gouy phase was acquired by the passage of the mode Vh through the π-converter. The intensity distribution of the interference patterns can be simulated by applying the matrix formalism to the optical circuit showed in Fig. 2. For this case, the results are shown in Fig. 3e and f. As we can see, there is a good agreement between the experimental results and the simulation with respect to the intensity distributions.

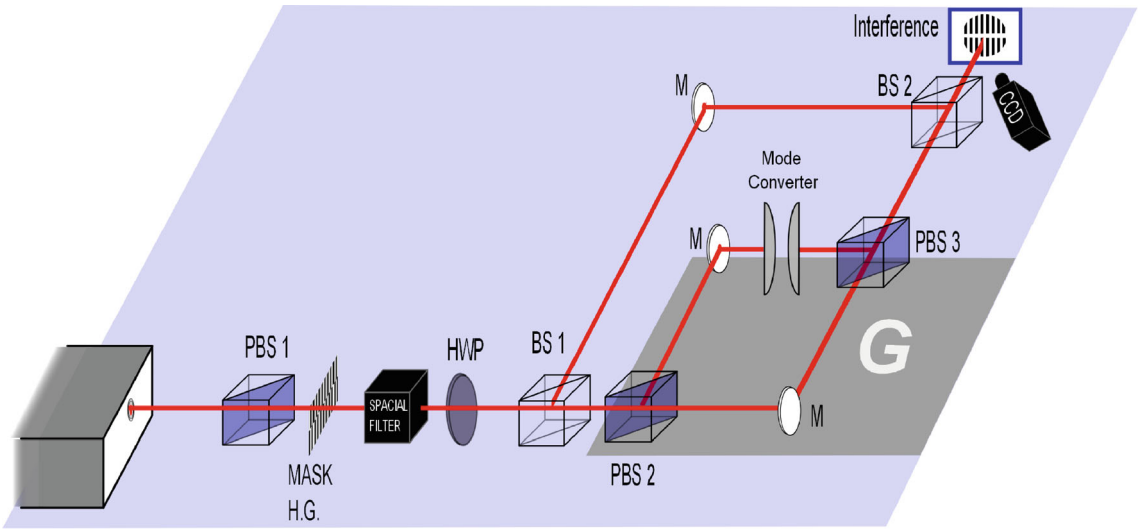

Fig. 2 Experimental setup

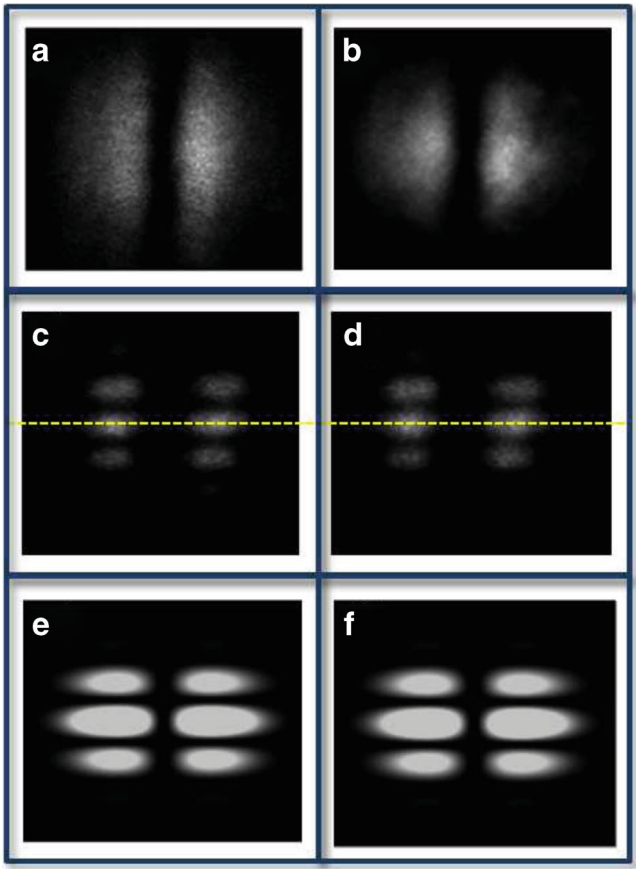

Fig. 3 Intensity distribution of modes *Hh* (**a**) and *Vh* (**b**). Interference patterns of modes *Hh* (**c**) and *Vh* (**d**). Interference patterns simulations of modes *Hh* (**e**) and *Vh* (**f**). *Dashed line* is a guide for the eyes

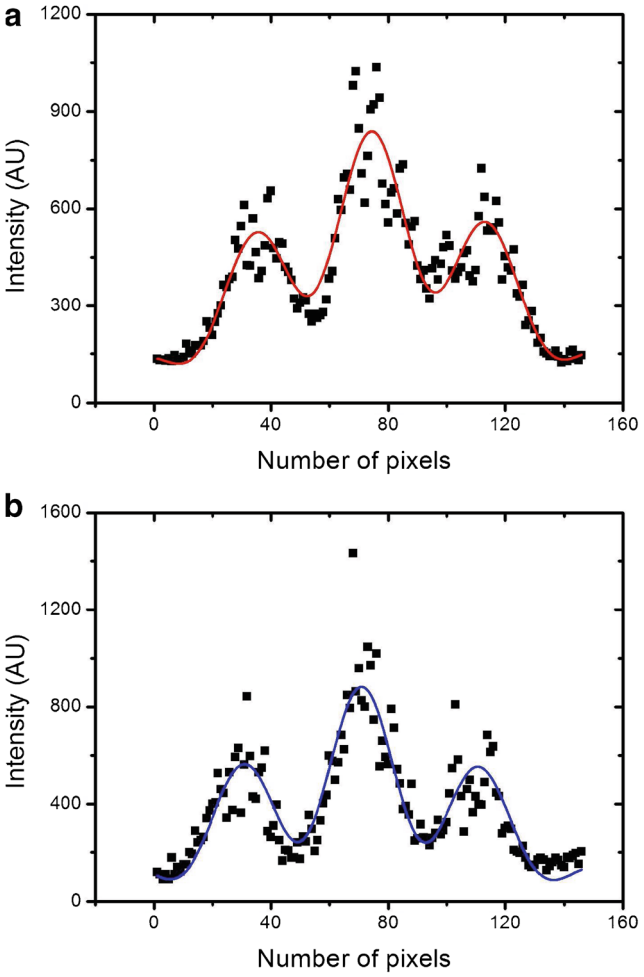

Fig. 4 Plot of a transverse line from the interference patterns corresponding to the mode *Hh* (**a**) and *Vh* (**b**). *Solid lines* are nonlinear fitting

In order to quantify the relative phase, a transverse line from each interference pattern was plotted. Figure 4a shows the result corresponding to the mode Hh, whereas Fig. 4b corresponds to the mode Vh. The solid lines are nonlinear fits, showing that the phase difference between these states is practically zero, in good agreement with the expected value. The nonlinear fit is based on the interference pattern between two gaussian beams, modeled by the equation $y(x) = A_0[1 - \mu cos(kx - \delta)]e^{-(x-x_0)^2/w_0}$, where A_0, x_0, w_0, μ, k, and δ are free parameters to fit the experimental data. By applying this fitting into our results, we obtain the spatial frequency k to measure the phase shift in terms of $k\Delta x$, where Δx is the relative spatial displacement of the interference patterns.

The second data set corresponds to the intensity profiles for the modes Hv and Vv. The results are shown in Fig. 5a (Hv) and b (Vv). The corresponding interference patterns are shown in Fig. 5c and d, where the dashed line is also a guide to the eyes. In this case, it is observed that there is a relative Gouy phase due to the passage through the π-converter. Note that a dark fringe is in the center of Fig. 4c whereas a bright fringe appears in the center of Fig. 5d, indicating a phase difference of π between the modes. The results for the simulation are shown in Fig. 5e and f, showing the presence of the same relative phase, in good agreement with the experimental results.

The transverse line from each interference patterns was also obtained in order to quantify the phase difference between these modes. The results are shown in Fig. 6. The profile relative to the mode Hv is shown in Fig. 6a, and the profile relative to mode Vv is presented in Fig. 6b. Performing the same nonlinear fitting, we have found a phase difference of 3.19 rad, in good agreement with the expected $\pi\ rad$ phase difference.

From these results, we verify the conditional phase shift in the first-order Hermite-Gaussian beam. The input modes were switched just by rotating the HWP, keeping the alignment of the reference beam for each data set. The robustness of our proposal is based on the fact that the Gouy phase is imprinted only on the proper transverse mode.

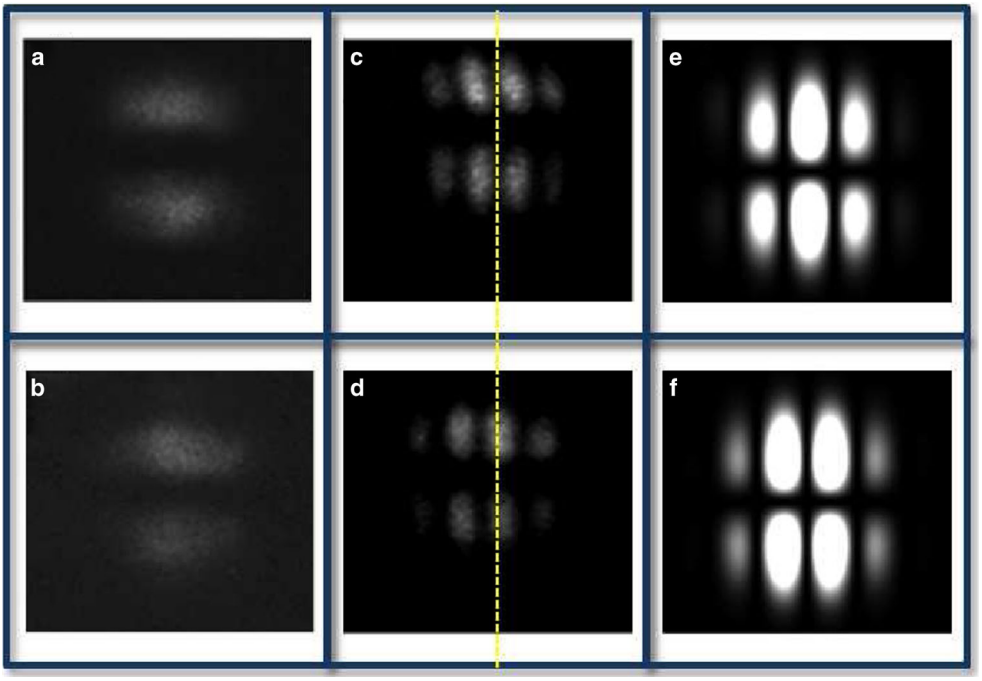

Fig. 5 Intensity distribution of modes Hv (**a**) and Vv (**b**). Interference patterns of modes Hv (**c**) and Vv (**d**). Interference patterns simulations of modes Hv (**e**) and Vv (**f**). *Dashed line* is a guide for the eyes

Even though our experiment was performed using an intense laser beam, the results show that it is possible to control the phase of a particular classical state of the electromagnetic field, described in terms of polarization and spatial mode degrees of freedom. As a consequence, our scheme is a good candidate to implement a conditional phase gate for photonic qubits in the context of the linear optical quantum computing (LOQC) [22]. In the next section, we present a proposal for this implementation, taking into account the necessary changes on the experimental realization.

4 Application: Quantum Phase Gate

Quantum logic gates are important elements for implementing quantum communication protocols and quantum algorithms [20]. In a two-qubit system, quantum logic gates can be used to perform conditional operations, where the state of one qubit controls the state of the other one. To implement such gates, different physical systems have been studied. In particular, optical systems have been extensively studied exploiting different degrees of freedom of the electromagnetic field, for instance, polarization and orbital angular momentum [21].

Concerning the LOQC, the use of single photons can be seen as an advantage for the decoherence problem, due to the weak interaction between photons and environment. On the other hand, the implementation of quantum algorithms is not easily scalable [22]. In fact, the number of optical components used to implement some computational operation grows exponentially as a function of the number of qubits. Knill, Laflamme, and Milburn have developed a protocol where LOQC becomes scalable using beam splitters, phase-shifters, and photodetectors associated with detection feedback [23]. Here, we are considering a non-scalable two-qubit LOQC to present how our optical circuit can be applied to implement a quantum phase gate.

The two-qubit quantum phase gate ϕ [20] can be defined as

$$G(\phi)\,|m,n\rangle \;=\; e^{i\phi mn}|m,n\rangle, \tag{8}$$

where $G(\phi)$ is the gate operation, $m,n = 0,1$. Note that the ϕ phase is acquired by the state only when $m = n = 1$. In order to implement a quantum phase gate, we need a system able to give a conditional difference of phase in the two-qubit state.

Let us discuss the quantum counterpart of our approach. As discussed in Section 2, our circuit is only composed of passive components. Therefore, the quantum behavior can be observed only if the input state is prepared in a single photon state of the electromagnetic field. Different degrees of freedom of a single photon can be used to prepare a two-qubit state.

In our proposal, the single-photon input state is prepared possessing a linear polarization and transverse mode HG. The qubits are encoded in polarization and transverse mode. Following the usual notation, $H-$polarization and $V-$ polarization are associated with the states $|\,0\rangle$ and $|\,1\rangle$, respectively. For the first-order Hermite-Gaussian mode, we associate $HG_{1,0}$ (referred as h) to the state $|0\rangle$ and $HG_{0,1}$ (referred as v) to the state $|1\rangle$. Regarding the phase gate rules, only the state $|11\rangle \;=\; |Vv\rangle$ acquires the π phase

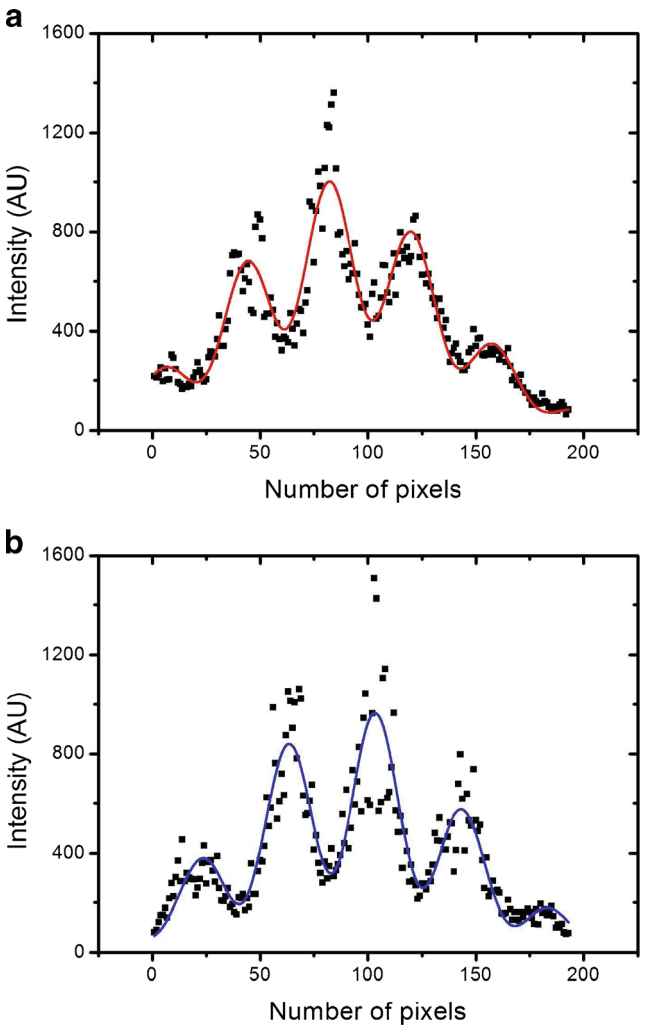

Fig. 6 Plot of a transverse line from the interference patterns corresponding to the mode *Hv* (**a**) and *Vv* (**b**). *Solid lines* are nonlinear fitting

passing into the mode converter. Therefore, the controlled phase shift presented in Section 2, with the input state corresponding to two-qubit state prepared as mentioned above, works exactly as a quantum phase gate, as shown in the truth table presented in Table 1. It is important to mention that our scheme allows to implement a general phase gate by controlling the distance between the cylindrical lenses.

By attenuating a polarized laser beam to the photo-counting regime, we can perform measurements where the quantum effects of the electromagnetic field with two degree of freedom can be observed. All input sates needed to verify the truth table associated with the phase gate can be obtained by rotating the HWP and the mask. By a linear scanning of avalanche photo-counting detectors, it is possible to measure the interference patterns. The same nonlinear fitting can be employed in order to quantify the difference of phase shift. Our experimental results, presented in Section 3, can be seen as a classical limit of the quantum experiment.

Table 1 Truth table of the quantum phase gate

Input	Output
$\|Hh\rangle = \|00\rangle$	$\|00\rangle$
$\|Hv\rangle = \|01\rangle$	$\|01\rangle$
$\|Vh\rangle = \|10\rangle$	$\|10\rangle$
$\|Vv\rangle = \|11\rangle$	$e^{i\pi}\|11\rangle$

5 Conclusion

In conclusion, we have proposed and experimentally demonstrated a device for implementing a conditional π-phase shift applied on Hermite-Gaussian beams. Our scheme is based on an optical circuit where a Gouy phase is imprinted depending on the polarization and transverse spatial modes states. The experimental results show a good agreement with the simulation of the optical circuit. It is worth to mention that a ϕ-phase shift can also be implemented by changing the separation of the cylindrical lenses of the mode converter.

As an application, a two-qubit quantum phase gate can be implemented by encoding the qubits on the transverse spatial modes and polarization. The corresponding truth table can be verified by attenuating the laser beam and performing the measurements in the photo-counting regime. To the best of our knowledge, two-qubit single photon states have never been exploited for implementing phase gates. For this reason, our proposal adds a new contribution on the scenario of optical implementation of quantum gates, where different degree of freedoms of the electromagnetic field are used to encode qubits.

Acknowledgments Funding was provided by Coordenação de Aperfeiçoamento de Pessoal de Nível Superior (CAPES), Fundação de Amparo à Pesquisa do Estado do Rio de Janeiro (FAPERJ-BR), and Instituto Nacional de Ciência e Tecnologia de Informação Quântica (INCT-IQ-CNPq).

References

1. K. Dholakia, N.B. Simpson, M.J. Padgett, L. Allen, Phys. Rev. A **54**, R3742–3745 (1996)
2. D.P. Caetano, M.P. Almeida, P.H. Souto Ribeiro, J.A.O. Huguenin, B. Coutinho dos Santos, A.Z. Khoury, Phys. Rev. A **66**, 041801 (2002)
3. S.P. Walborn, A.N. de Oliveira, S. Pádua, C.H. Monken, Phys. Rev. Lett. **90**, 14360 (2003)
4. A.C. Dada, J. Leach, G.S. Buller, M.J. Padgett, E. Andersson, Nat. Phys. **7**, 677–680 (2011)
5. Y.-H. Kim, Phys. Rev. A **67**, 040301 (2003)
6. M. Fiorentino, N.C. Wong, Phys. Rev. Lett. **93**, 070502 (2004)

7. S. Roychowdhury, V.K. Jaiswal, R.P. Singh. Opt. Commun. **236**, 419–424 (2004)
8. L.-P. Deng, H. Wang, K. Wang, J. Opt. Soc. Am. B **24**, 2517–2520 (2007)
9. C.E.R. Souza, A.Z. Khoury, Opt. Express **18**, 9207–9212 (2010)
10. A.N. de Oliveira, S.P. Walborn, C.H. Monken, J. Opt. B: Quantum Semiclass. Opt. **7**, 288–292 (2005)
11. C.E.R. Souza, C.V.S. Borges, A.Z. Khoury, J.A.O. Huguenin, L. Aolita, S.P. Walborn, Phys. Rev. A **77**, 032345 (2008)
12. E. Nagali, F. Sciarrino, F. De Martini, B. Piccirillo, E. Karimi, L. Marrucci, E. Santamato, Opt. Express **17**, 18745 (2009)
13. A.R.C. Pinheiro, C.E.R. Souza, D.P. Caetano, J.A.O. Huguenin, A.G.M. Schmidt, A.Z. Khoury, J. Opt. Soc. Am. B **30**, 3210–3214 (2013)
14. M.J. Padgett, J. Courtial, Opt. Lett. **24**, 430–432 (1999)
15. C.R. Gouy, Acad. Sci. Paris **110**, 1251–1253 (1890)
16. A.E. Siegman, *Lasers* (University Science Books, Sausalito, 1986)
17. S. Feng, H.G. Winful, Opt. Lett. **26**, 485–487 (2001)
18. M.W. Beijersbergen, L. Allen, H.E.L.O. van der Veen, J.P. Woerdman, Opt. Commun **96**, 123 (1993)
19. L. Allen, J. Courtial, M.J. Padgett, Phys. Rev. E **60**, 7497 (1999)
20. M.L. Nielsen, I.L. Chuang, *Quantum computation and quantum information* (Cambridge University Press, Cambridge, 2000)
21. A. Mair, A. Vaziri, G. Weihs, A. Zeilinger, Nature **412**, 313–316 (2001)
22. G. Chen, D.A. Church, B.G. Englert, C. Henkel, B. Rohwedder, M.O. Sccully, M.S. Zubairy, *Quantum compution devices, principles, devices, and analysis* (Chapman & hall/CRC, New York, 2007)
23. E. Knill, R. Laflamme, G.J. Milburn. Nature **409**, 46 (2001)